Copyright Warning & Restrictions

The copyright law of the United States (Title 17, United States Code) governs the making of photocopies or other reproductions of copyrighted material.

Under certain conditions specified in the law, libraries and archives are authorized to furnish a photocopy or other reproduction. One of these specified conditions is that the photocopy or reproduction is not to be "used for any purpose other than private study, scholarship, or research." If a, user makes a request for, or later uses, a photocopy or reproduction for purposes in excess of "fair use" that user may be liable for copyright infringement,

This institution reserves the right to refuse to accept a copying order if, in its judgment, fulfillment of the order would involve violation of copyright law.

Please Note: The author retains the copyright while the New Jersey Institute of Technology reserves the right to distribute this thesis or dissertation

Printing note: If you do not wish to print this page, then select "Pages from: first page # to: last page #" on the print dialog screen

ABSTRACT

THE EFFECTS OF DESIGN PARAMETERS ON THE NEURAL RECORDINGS WITH MICRO-ECoG ARRAYS

by
Manan Amish Sethia

In the field of neural prosthetics, electro-cortico-graph (ECoG) arrays are commonly used to record neural activity of the brain cortex both in animal and human subjects. A finite element model (FEM) was developed to simulate the electric field generated by a single neuron in the rat brain cortex and a micro ECoG array (µECoG) placed on the pia surface for recording the neural signal. The neuron was simulated as a dipole current source with a magnitude of 1µA and placed at three different depths in the motor cortex corresponding to different layers under the µECoG array. The array design was a grid of 8x8 circular contacts with a contact pitch of 500 µm and via holes between the recording contacts. The main hypothesis was that the presence of these holes should have significant impact on the amplitude and selectivity of the neural signals depending on the depth of the source in the cortex. The sizes of via holes were set to 20, 50, and 200 µm to study their effect on the recorded potentials. These results show that the recorded signal amplitudes drop at the location of the via holes and the overall amplitudes also decreases at the contact sites as compared to the design without the holes. The larger the hole size, the larger the effect on the signal amplitude. Furthermore, the simulation results supported the hypothesis that greater potential differences were created due to the presence of holes in µECoG arrays and improved the selectivity of neural recordings.

THE EFFECTS OF DESIGN PARAMETERS ON THE NEURAL RECORDINGS WITH MICRO-ECoG ARRAYS

by
Manan Amish Sethia

A Thesis
Submitted to the Faculty of
New Jersey Institute of Technology
in Partial Fulfillment of the Requirements for the Degree of
Master of Science in Biomedical Engineering

May 2021

APPROVAL PAGE

THE EFFECTS OF DESIGN PARAMETERS ON THE NEURAL RECORDINGS WITH MICRO-ECoG ARRAYS

Manan Amish Sethia

Dr. Mesut Sahin, Thesis Advisor — Date
Professor of Biomedical Engineering, NJIT

Dr. Xianlian Alex Zhou, Committee Member — Date
Associate Professor of Biomedical Engineering, NJIT

Dr. Antje Ihlefeld, Committee Member — Date
Assistant Professor of Biomedical Engineering, NJIT

BIOGRAPHICAL SKETCH

Author: Manan Amish Sethia

Degree: Master of Science

Date: May 2021

Undergraduate and Graduate Education:

- Master of Science in Biomedical Engineering,
  New Jersey Institute of Technology, Newark, NJ, 2021
- Bachelor of Engineering in Instrumentation & Control Engineering,
  Gujarat Technological University, Gujarat, India, 2016

Major: Biomedical Engineering

ॐ

|| જય જિનેન્દ્ર ||

|| શ્રી ગણેશાય નમઃ ||

“I worship you before beginning to write my thesis, Remover of Obstacles”

To my parents, to my wife, my family members and to all my friends

ACKNOWLEDGEMENT

I would like to thank Dr. Mesut Sahin for being my advisor, for his immensely helpful personality and guiding me towards the right direction, providing me an opportunity to learn COMSOL Multiphysics software, and teaching me the art of neuroscience. His lectures and notes have made me capable to understand the physics embodied in neuro-prostheses and I am sure that learning finite element analysis would surely benefit me in my career ahead. I would also like to thank Dr. Xianlian Alex Zhou and Dr. Max Roman for teaching me ANSYS software and giving me insights on methods to apply boundary conditions and meshing techniques. I further extend my gratitude towards Dr. Alev Erdi for believing in me to be her teaching assistant in Fundamentals Engineering Design class for undergraduate course, that helped me polish my skills with MATLAB programming. I am very grateful to Dr. Antje Ihlefeld for being my committee member on thesis. Fellow Ph.D students, Ozan Cakmak, Esma Cetinkaya, Qi Kang and Alex Tzalvaros also deserve appreciation for the in-lab discussions and informative sessions that helped me in thesis. I would like to thank Dr. Saikat Pal for taking out his time to help me troubleshoot the software related errors. Last but not the least I extend my thanks to fellow colleague Darshan Shah for his valuable insights into programming and hardware limitations.

TABLE OF CONTENTS

TABLE OF CONTENTS
(Continued)

LIST OF TABLES

LIST OF FIGURES

LIST OF FIGURES
(Continued)

LIST OF SYMBOLS

©	Copyright
µ	Micrometer (10^{-6})
mm	Millimeter (10^{-3})
m	Meter (10^{1})
S	Siemens
σ	Electrical Conductivity
Φ	Diameter
V_A	Voltage at point A
V_B	Voltage at point B
SS	Spatial Selectivity
®	Registered
~	Approximately

LIST OF DEFINITIONS

Amplitude	It is the maximum value or peak value of voltage attained in a recording electrode.
Electric Dipole	It is a pair of equal and opposite electric charges.
Contact pitch	Distance between the center of two contact electrodes.
Electrical Conductivity	It is a property of any specified material that determines the degree of passage of electricity through that material. Here, it is expressed in (S/m).
Spatial Selectivity	It is defined as the ratio of the potential difference between the voltages induced by those two neurons to the voltage of the neuron that is located closer to the recording site.
Signal Noise Ratio	Signal-to-noise ratio is defined as the ratio of the power of a signal to the power of the background noise.

CHAPTER 1

INTRODUCTION

The importance of neural recording is to retrieve data from neurons and utilize it to combat against the movement related disorder such as Epilepsy or Parkinson's disease as well as other traumatic injuries or brain related diseases. As it is now evident that µECoG are more efficient then ECoG due to its higher spatial resolution capability, we put efforts into discerning the efficacy of various commercially available µECoG designs. µECoG arrays also belong to a group of tools utilized in brain computer interfaces (BCI) which are designed to decode volitional components in the recorded signals. We developed a realistic rat brain model to apply finite element methods to compute a study of electric field. We then incorporated different µECoG designs into the study and analyzed their impacts on the recorded voltage profiles in three different sets of simulation. The BCIs, the rat brain and its properties, nuances in µECoG models, its applications, and finite element methods are all described in the first few chapters in their respective order. Then, the simulation results are presented, and followed by discussion. The last section summarizes the future directions.

CHAPTER 2

BRAIN COMPUTER INTERFACES

The function of a BCI is to record the brain activity and extract signal features in order to restore or improve the lost motor function in a person with paralysis that results from neural injury or disease. There are several techniques to interface with brain signals, they are categorized on their degree of invasion: non-invasive, semi-invasive and invasive.

Electroencephalography (EEG) and Magnetoencephalography (MEG) are the non-invasive methods. As the brain produces electrical signals, the sensors attached to scalp measures the electric field in former and magnetic field in latter. ECoGs are considered to be semi-invasive, but requires craniotomy as they are placed on the dura mater of the brain and provides a significant coverage of area of the cortex, forming a grid layout and ranges from 4 to up to 256 contact sites. The most invasive procedure consists of implanting penetrating electrode arrays into the parenchyma of the brain to read the potential voltages within the cortex. The spatial resolution of recording the signals is directly related to the degree of invasiveness. The deeper the electrode, the better is the spatial resolution.

BCIs interpret the neural signals that are detected using electrodes with varying degrees of invasiveness (EEG, ECoG or penetrating arrays) and transfer them into commands that control an output device such as a robotic arm. The methods of interfacing with the cerebral cortex and their corresponding electrodes can be mainly divided into three categories: external scalp recordings from electroencephalography (EEG), surface cortical recordings from electrocorticography (ECoG or micro ECoG), and intracortical recordings from within the cortex and brain parenchyma using penetrating electrode arrays.

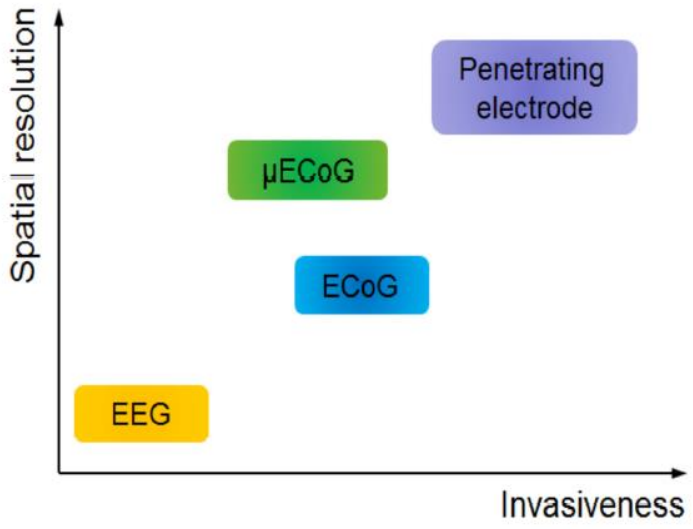

Figure 1.1 Spatial resolution versus invasiveness for various types of neural electrodes. *Source: [1]* Micro-ECoG has a balanced spatial resolution and invasiveness.

Initial attempt in BCIs laid the foundations where neuronal signals were acquired and processed on computer in non-human primates [2]. An implanted microelectrode array in primary cortex of a patient with tetraplegia led the patient to operate television and control prosthetic hand by reading the signals acquired from the electrode array [3]. Subjects were able to spell words on an output monitor when the recorded signals from an ECoG were translated by a BCI [4]. Activity of neurons in motor cortex of a monkey were decoded into a signal that could replicate the movements of limb [5]. Researchers have demonstrated that neural signals in rats [6] could be used to position the robot arm to obtain water. Primates [7] could learn to make one-dimensional and three-dimensional movements via the recorded brain signals.

CHAPTER 3

MICRO-ELECTRO-CORTICO-GRAM

µECoG array is an important tool to diagnose and treat disorders like epilepsy and monitor neuronal activity without penetrating the brain parenchyma, placed on the dura mater or subdurally on the pia. They are commercially available with metal contacts with varying size, inter-contact distance (pitch), number of contacts as a grid on a non-conductive substrate material such as silicone, parylene-C, or polyimide [1]. The via holes through the substrate is usually included into the design to allow passage of interstitial fluid from one site to the other, and minimize the compression of the micro vessels under the substrate. However, the electrode array designs are mostly based on subjective experience of the investigators and putative information that is believed to best match the application in consideration. Particularly the size of the via holes must make a significant effect on the recorded signal amplitudes since they provide a passage through a non-conductive material that forms an electric barrier between the two sides of the array. In this thesis, we looked into the issue using the FEM simulations to have an insight as to how the substrate sizes and the size of the via holes affect the recorded signal amplitudes from a neuron located in the gray matter of the cortex.

Micro-electrocorticogram (µECoG) arrays have become more favorable due to their ability to provide higher temporal and spatial resolution. The anticipation of customized µECoG for a specific application intrigued us to experiment and analyze a few µECoG designs and their sizes. The interelectrode spacing (contact pitch) in a µECoG was a factor in correlating the recorded signals for human subjects and mouse [8]. Flexible µECoG electrode array was used for long-term recording from the rat auditory cortex [9],

which had a 27 µm thick substrate, contacts arranged in 8 x 8 grid, and disk shaped contacts with a diameter of 200 µm. The photolithography allows the fabrication of varying sizes, shapes, and patterns for the contacts [10]. A smaller size of contact diameter and contact pitch in µECoG provides more neural information than a standard ECoG array when used to record from the same cortical region [11] However, there is no significant study on the µECoG designs with respect to the size of substrates and presence of via holes regarding their impact on the voltage profiles recorded at the contact sites. Thus, the computational modelling and insight gained from such analyses can provide valuable information and guide the design of these devices for research and the clinic diagnostic applications.

3.1 Design layout

Industrial manufacturers like CorTec [12] and NeuroNexus [13] have developed numerous types of array degins customized for specific applications of neural recordings and stimulation. The array design in this study included four different substrate sizes (Table 1) and varying via hole diameters Φ0 µm, Φ20 µm, Φ50 µm and Φ200 µm in a µECoG with disk shaped contacts of Φ100 µm diameter.

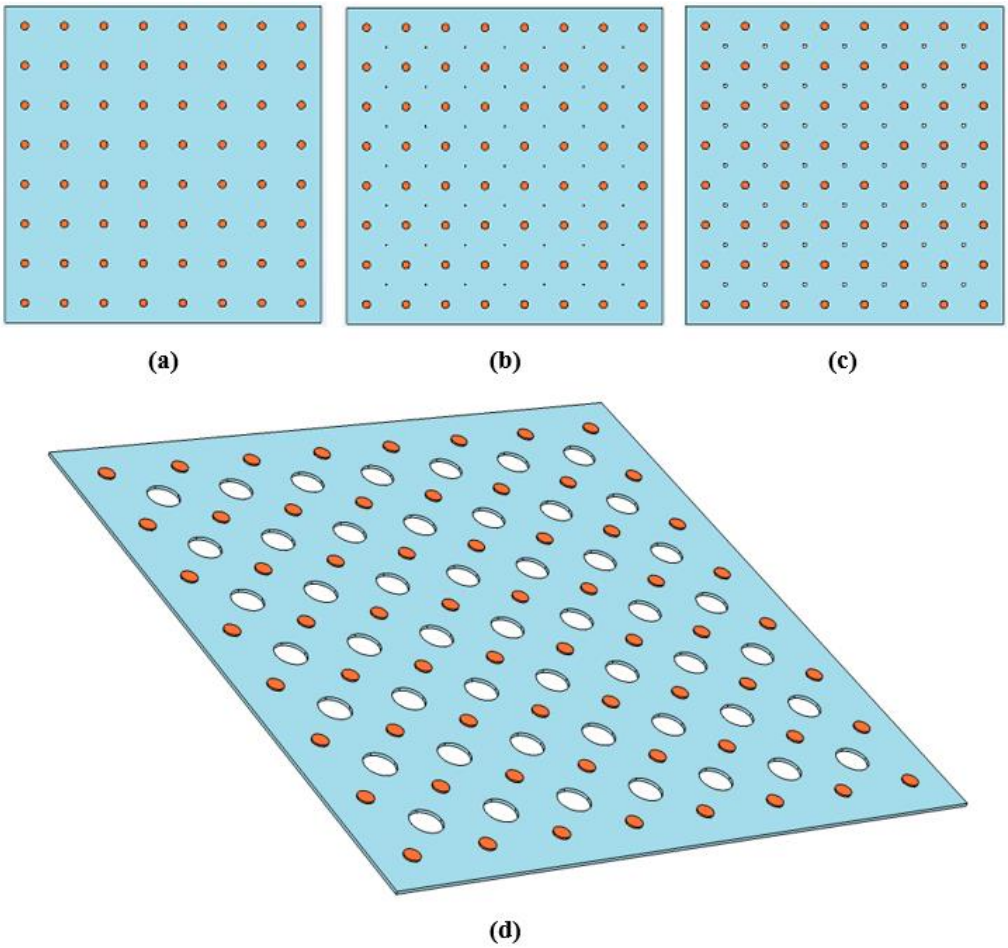

Figure 3.1 Layout of the µECoG with substrate size of 4 x 4 mm, (a) no holes, (b) Φ20 µm, (c) Φ50 µm and (d) Φ200 µm and contacts (orange shade) Φ100 µm.

3.2 Material Properties

Various configurations specified above are employed with a wide range of combining materials to achieve a specific type of neural recordings. The important parameters for these materials are electrical conductivity and biocompatibility. Moreover, properties can be tweaked by modifying their surfaces.

Iridium (Ir): Cytotoxicity assay test results elicit that iridium, although less so than gold and indium tin oxide, promotes cell growth and has no inhibitory effects on cells after being in contact for up to 72 hours, when compared to a control surface i.e. a well in a multidish

polystyrene tissue culture plate, surface treated for optimum conditions for cell attachment and growth[14]. Nonetheless, it is often used as Iridium oxide or in its sputtered form due to its increased charge injection capacity. However, it is less flexible.

Platinum (Pt): Pt is a good choice for the electrode contacts with their superior charge storage capacity that increases with surface roughness and the impedance becomes lower. The angle sputtering deposition at 30°, 45° and 90° was done and it confirmed adsorption of protein layer whereas degradation tests proved that it is chemically inert [15]. Pt as a noble metal is stable electrochemically, and optimal for making small metal contacts resulting in high resolution arrays.

Graphene: It is referred as a two-dimensional allotrope of carbon, due to the arrangement of atoms. It is transparent, flexible and produces low noise. 50 µm electrode was engineered that attained 5–6 fold improvement in signal-to-noise ratio (SNR) and 100 fold reduction in electrical interference noise [16].

Indium tin oxide (ITO): Similar to Ir, cytotoxicity assay shows that ITO and gold (Au) has no inhibitory effects on cells and ellipsometry results suggest that ITO had the thinnest layer of protein adsorbed and also promotes cell growth [14]. Moreover, it is also transparent and flexible.

Bioresorbable Silicon: As the name suggests, this material can prevent second surgery for extraction of the electrode array post-recording in neurological studies where this material tend to disappear in fluids after a definite amount of time, thanks to the contemporary advances in the silicon devices that led to the innovation of its bioresorbable nature [17]. The material is described as a ultrathin silicon nanomembrane. A thin and flexible electrode array was developed where Si contacts were used for direct neural interface and

bioresorbable polymer poly(lactic-co-glycolic acid, PLGA, thickness ~30 μm) served as the substrate, effectively utilized for recording from rat cortex [18].

Polyimide: A biocompatible device, suitable for substrate due to its electrical insulation, mechanical flexibility and biocompatibility [19].

Table 3.1 Material Properties and Geometry of μECoG Array

Attribute	Dimension	Material Properties	Electrical conductivity (σ)
contact diameter	100 μm	Platinum/Iridium	4×10^6 S/m
contact pitch	500 μm		
No. of contacts	8 x 8 contacts		
substrate dimensions	0.5 x 0.5 mm 1 x 1 mm 2 x 2 mm 4 x 4 mm	Polyimide	6.667×10^{-16} S/m
Via holes	20 μm 50 μm 200 μm	N/A	N/A
substrate thickness	20 μm		

CHAPTER 4

RAT BRAIN

A rat brain is a unification of ten layers that comprise of membranous sheath and tissues. Among this framework are located the three meninges: dura mater, arachnoid mater and pia mater. The arachnoid mater and pia mater are separated by a thin transparent membrane referred as cerebrospinal fluid or sub-arachnoid space. These meninges provide a protective coating and contribute towards the supportive foundation of central nervous system. Dura mater is a thick and dense membrane, while arachnoid and pia are relatively thinner membranes, but impermeable to fluid. Neurons are located beneath the pia mater, deep down in gray matter (GM), and glial cells that feed nutrients and energy to neuron cells. Since our simulations were based on electrostatic studies, our focus was specifically on pyramidal neurons located in the layer V of GM [1].

A FEM was designed to mimic a rat brain. The model was divided in ten isotropic layers representing air, scalp, skin, skull, dura mater, arachnoid, sub-arachnoid or cerebrospinal fluid (CSF), pia mater, gray matter and the white matter (Table 4.1), that were assigned individual electrical conductivities obtained from publication.

Table 4.1 Brain Layer Thickness and Corresponding Electrical Conductivity Values

Rat Brain Model			
Layer	Thickness (μm)	Electrical conductivity (σ) in (S/m)	References
Air	100	$1x10^{-15}$	
Scalp	500	0.2	[20]
Skin	500	0.05	
Skull	1000	0.02	[21]
Dura	100	0.03	[22]
Arachnoid	75	0.03	
CSF	100	1.8	[23]
Pia	25	0.23	
Gray	1800	0.23	[24]
White	1800	0.6	[25]

4.1 Neural Stimulation and Recording

There are other techniques applied for studies related to transcranial current stimulation in a realistic head model of the rat, where MRI data from a living rat was acquired to perform finite element analysis (FEA). The brain layers in that model were divided into bone, CSF and brain and electrical conductivities were averaged to that of human values [26]. Another rat model was developed by concentric spheres defining scalp, bone, CSF and gray matter, accompanied by insertion of a silicon-based microelectrode. However, the main emphasis of the study was on the signal-to-noise ratio (SNR) of the recordings, which was calculated for different contact sizes [27].

In our case, we introduced a dipole current source with a magnitude of 1 μA to mimic a neuron. The dipole sources were 50 μm apart and positioned vertically in the gray matter. The simulations were performed for three depths: 500 μm, 1000 μm and 1500 μm of the neuron from the pia surface. Voltage profiles were also simulated for the cases of no via holes and in the absence of an electrode array for comparison.

CHAPTER 5

FINITE ELEMENT ANALYSIS

COMSOL Multiphysics version 5.4 [28] was used to design the rat brain model and μECoG models. Finite element modeling and analysis is an important computational tool in neural engineering to simulate neural excitation with implanted electrodes or with surface electrodes. The finite element method is often used to study electric fields in volume conductors and continues to emerge as a useful tool in the field of neuroscience. In this study, FEA was done to demonstrate the effect on voltage profiles at recording site for three different via hole sizes. Layer thickness and electrical conductivity values were obtained from literature for the rat brain motor cortex. COMSOL Multiphysics was the software package tool used to perform the FEA and study the post-processing results with proper boundary conditions.

5.1 Finite Element Modelling

5.1.1 Geometry

A brain model 10x10x6.1 mm consisting of ten layers, which can be better appreciated in figure 5.2, was incorporated with an inner box of 5x5x2.5 mm that was included for keeping a higher mesh resolution around the μECoG array and the neuron.

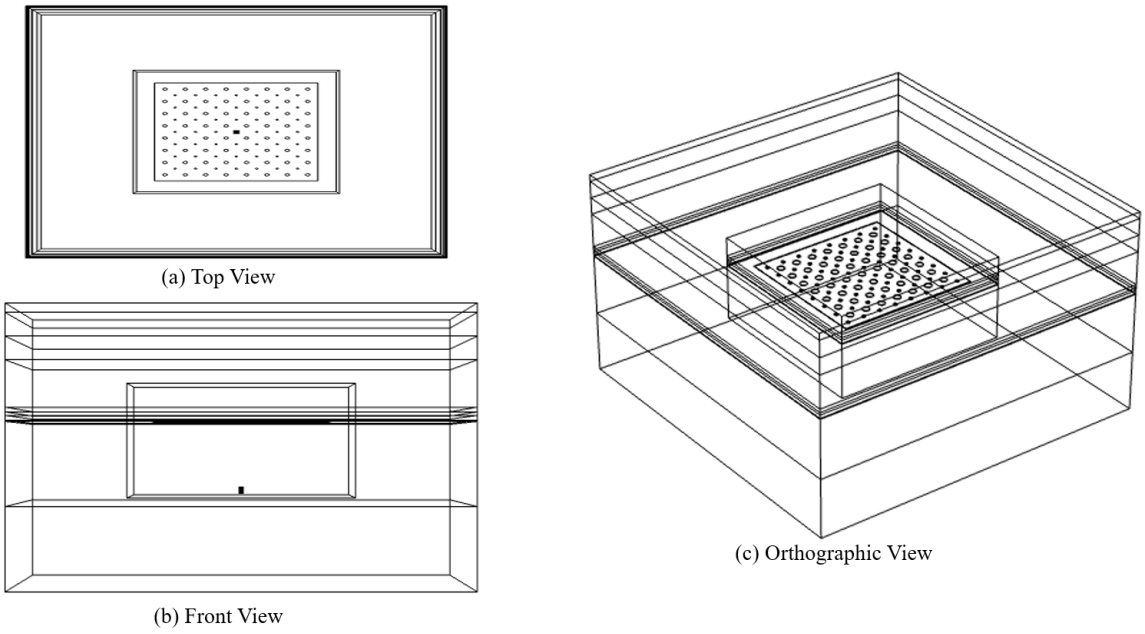

Figure 5.1 A simplified FEM for studying potential fields across the rat brain cortex recorded with a µECoG (Orthographic wireframe view).

5.1.2 Boundary Conditions

Appropriate material conductivity values from Table 4.1 were assigned to corresponding layers in Figure 5.2 and to the inner box layers that correlated with layers of the model. Boundary conditions were applied to the model by assigning ground terminal to all the outer boundaries of the model except the top surface, which was by default assigned as an insulator (air). Initial electric potentials were set to zero volts (V), +1 µA to the upper point and -1 µA to the bottom point current source that mimicked the neuron.

Figure 5.2 Various layers of the model with specific thicknesses and conductivities (see also Table 4.1).

Material	Selection
Air (mat1)	Domain 10
scalp (mat15)	Domain 9
skin (mat2)	Domain 8
skull (mat4)	Domains 7, 16
dura (mat5)	Domains 6, 15
arachnoid (mat...	Domains 5, 14
CSF (mat14)	Domains 4, 13
pia (mat6)	Domains 3, 12
gray (mat7)	Domains 2, 11
white (mat8)	Domain 1
neuron points (...	Points 858–859
polyimide (mat...	Domain 17
Platinum/Iridiu...	Domains 18–145

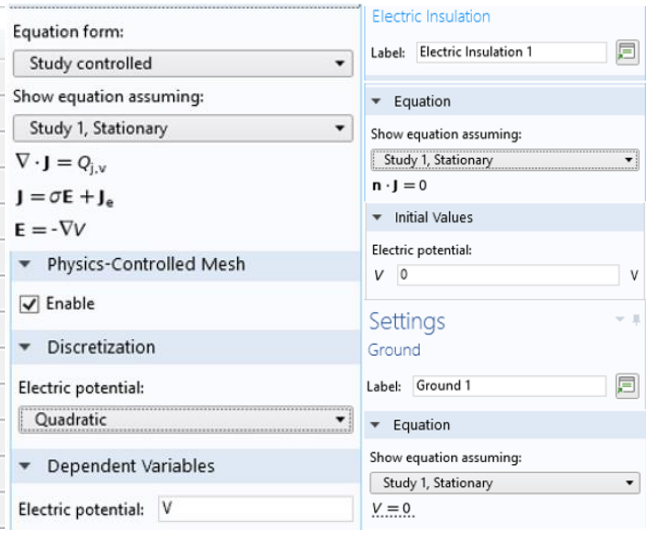

Figure 5.3 Material assignments and equation for boundary condition in the model.

5.1.3 Mesh

A small cubical 5x5x2.5 mm box constructed around the µECoG (Figure 5.4b) and the neuron and set to "extremely fine" level of mesh (element size 4 µm). The middle four

layers from pia to dura were set to “finer” mesh (element size 80 µm) and the gray matter, white matter and the top four layers were set to “fine” mesh (element size 200 µm).

Mesh elements type was free tetrahedral. Complete mesh consists of:

- 7232624 domain elements
- 917711 boundary elements
- 21153 edge elements

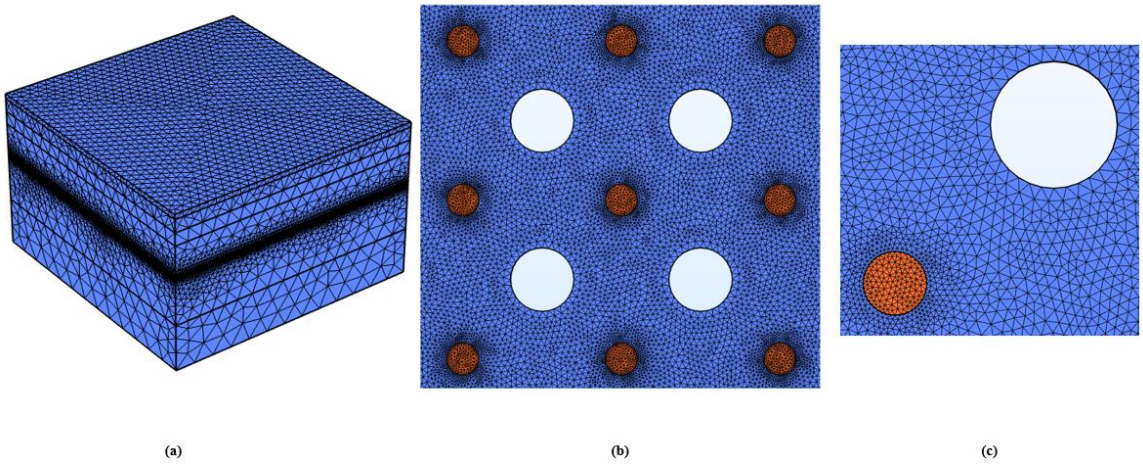

Figure 5.4 A detailed mesh view of the small box (a) and around the metal contacts (100 µm) and holes (200 µm) (b and c).

5.2 Post Processing

Voltages computed at all the elements of the 3D COMSOL model were exported to Matlab and voltage profiles at the bottom surface of the substrate were plotted. The presence of the metal contacts made very little difference in the voltage profiles, and thus the voltage at any point underneath the array could be thought of as a voltage measurement from an infinitely small hypothetical contact located at that point, if other contact configurations are to be considered.

As expected, the voltage drops exponentially by distance from the neuron that is simulated with a dipole current source (Figure 5.5). Near zero potentials are measured (blue areas) in regions where the anodic and cathodic potentials cancel out. The voltage field spreads further above the neuron than it does below the neuron due to the presence of a low-conductivity skull and the non-conductive air above the scalp. The electrode array (Figure 5.5a) also blocks the vertical flow of the current, which further reduces the voltage gradient in the vertical direction as compared to uniform flow in (Figure 5.5b) where μECoG is absent.

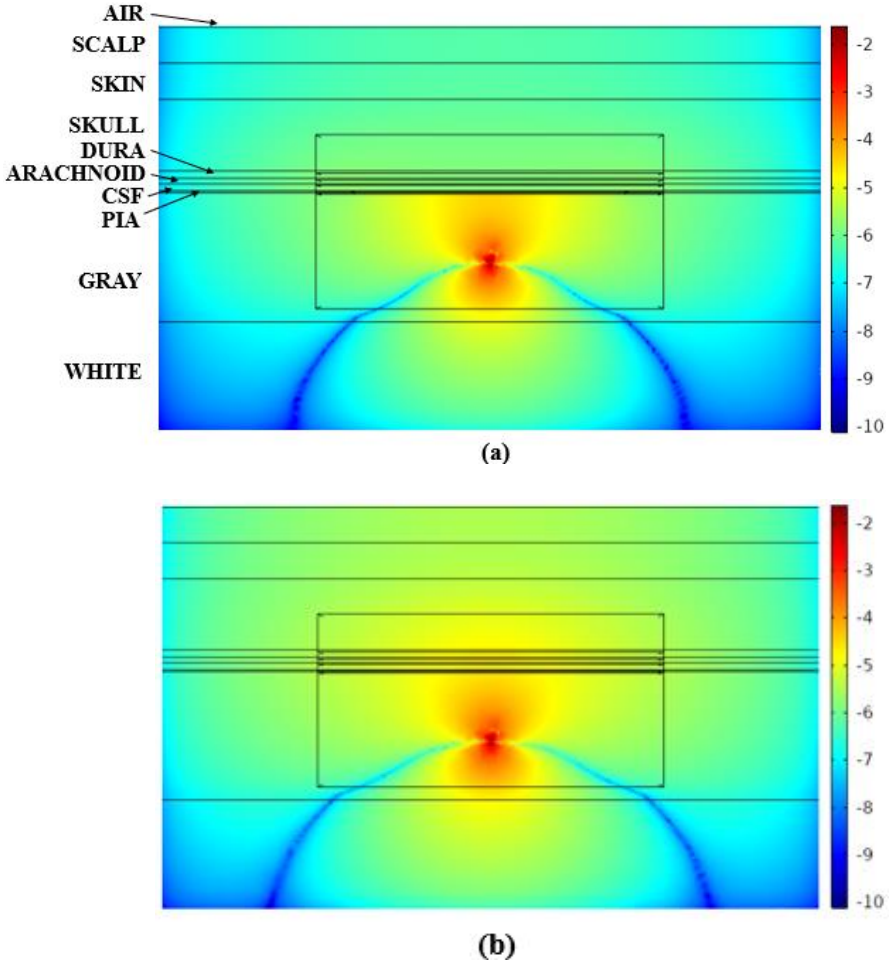

Figure 5.5 Voltage field in a vertical plane that goes through the center of the model. Absolute values of the voltages are shown on a logarithmic scale. The neuron is simulated with a dipole placed vertically. The small box delineates the region with extremely fine

mesh containing the array (a) and the neuron (b) without array. Both positive (above the neuron) and negative (below the neuron) voltages are shown on the same color scale because only the absolute values are used.

5.2.1 Voltage Profile For Different Substrate Sizes

In order to demonstrate the effect that the presence of a non-conductive substrate makes on the recorded voltages from a neuron located in the gray matter, the voltage profiles for different substrate sizes were plotted (Figure 5.6). Due to the presence of substrate, the voltage levels under the substrate increased and outside the substrate decreased (compare with the blue trace). The voltage profiles had sharp slope changes at the edges of the substrate. The peak voltage increased significantly with the substrate size and reached to ~34 µV for the 4 x 4 mm array (green trace), which was larger than twice the voltage recorded in the absence of the array (blue trace). For a substrate size (1 x 1 mm) that is in the same order as the neuron depth (1000 µm), the voltage increase was about 65%. This simulation shows that the presence and the size of a non-conductive array substantially impacts the voltages recorded at the contacts.

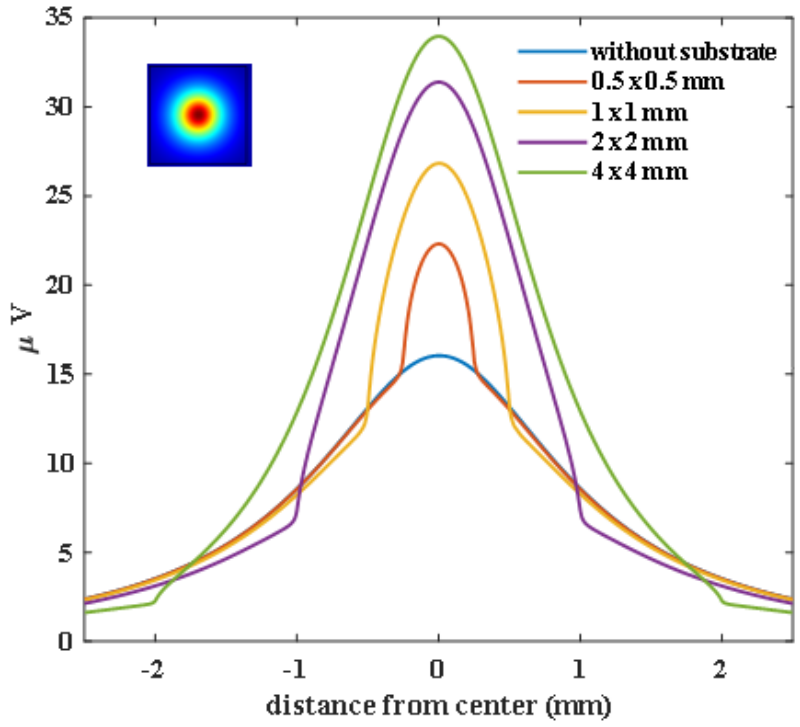

Figure 5.6 Diagonal voltage profile beneath the electrode array for varying substrate sizes as well as in the absence of a substrate. The recorded voltage increases with array size. The neuron is at a depth of 1000 µm from the substrate of the array and no via holes included.

5.2.2 Impact of Via Holes

The effect of the hole size was investigated by plotting voltages along the diagonal axis of the array for different neuron depths (Figure 5.7a). The relative voltage drop at the center of the holes were similar for all neuron depths, although the absolute values were smaller for deeper neurons. Due to presence of electrode contacts, horizontal steps are clearly visible in the profile because of their high electrical conductivity. Interestingly, the voltages at locations of the contacts that are away from the via holes were also affected and deviated from the voltage profiles of the "no holes" case by increasing amounts with the hole size (Figure 5.7b). The relative voltage decrease was the largest for the neuron depth of 500 µm.

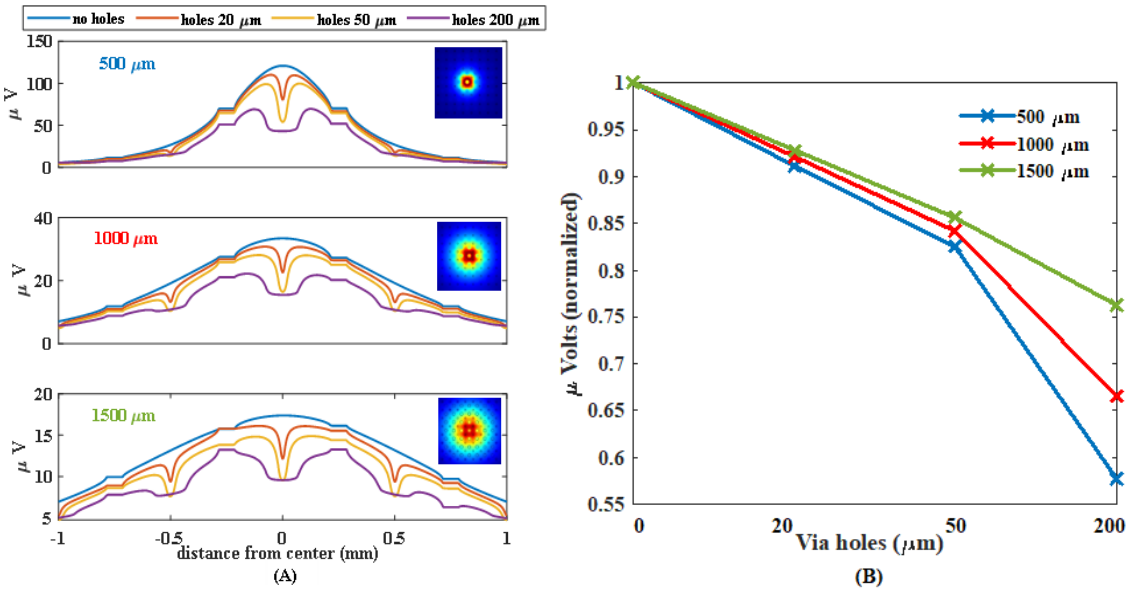

Figure 5.7 Voltage profiles recorded from neurons at three different depths (500 µm, 1000 µm, and 1500 µm), at the bottom surface and along the diagonal line of the array (4x4 mm) that goes through the centers of the holes and contacts (a). The neuron position was exactly beneath the geometric center of the array. Plot (b) shows the voltages recorded at the contact locations that are closest to the via hole at the array center. Each trace is normalized by the voltage of the substrate with no holes.

Next, the neuron was moved off-center and aligned with a contact on the diagonal axis in order to visualize the asymmetric effects of the array on the recorded voltages (Figure 5.7). The heat-plots in Figure 5.8 depicts the voltage profiles recorded at the bottom surface of the substrate at the contact level for all four variants of the hole size. The 3D mesh plot resembles a spongy bed like structure with a peak voltage at the coordinates of the source neuron. As the holes become larger, the sink-in effects at the holes become more visible while the overall voltage is decreasing (bottom panel). The asymmetry induced in the voltage distribution due to the array edges closer to the neuron are visible in the heat-plots of the bottom panel.

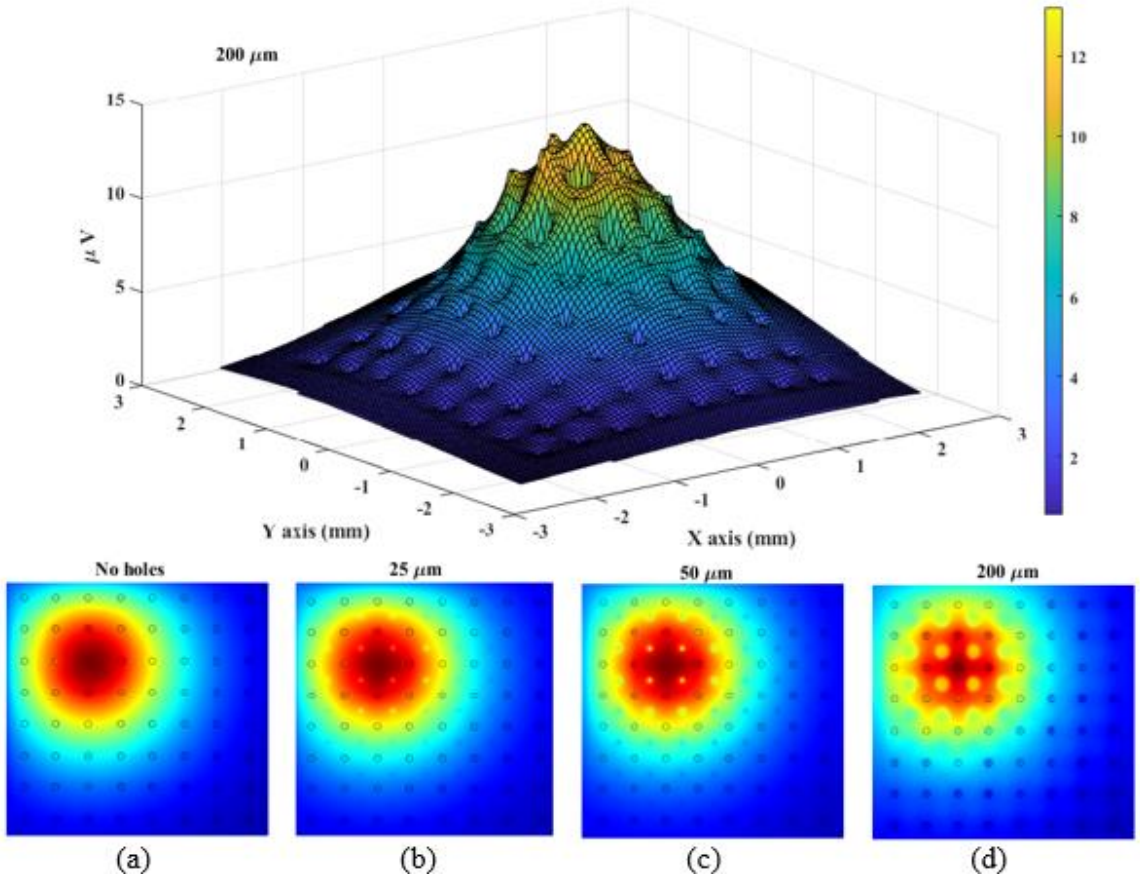

Figure 5.8 Top panel: Surface mesh plot depicting the effects of the holes (200 µm) on the voltage profile recorded at the level of the electrode contacts from a neuron located at the position marked by a white cross in the leftmost bottom plot and at a depth of 1500 µm. Bottom panel: 2D version of the voltage fields as in the top panel for different sizes of the via holes; no-holes (a), 20 µm (b), 50 µm (c), and 200 µm (d).

A similar analysis for all three neuronal depths was conducted in Figure 5.9. The voltage amplitudes decreased and spread wider for the neurons positioned deeper (500, 1000, and 1500 µm) into the gray matter from the pia surface. The via holes added to the substrate produced dips at corresponding positions in the voltage profiles and the size of the voltage drop increased with increasing hole size, as seen before in Figure 5.7a. Unlike the plots of Figure 5.7a, however, the asymmetric positioning of the substrate with respect to the neuron produced a slight asymmetric in the voltage profile, which was more pronounced with the neuron at 500 µm than deeper ones.

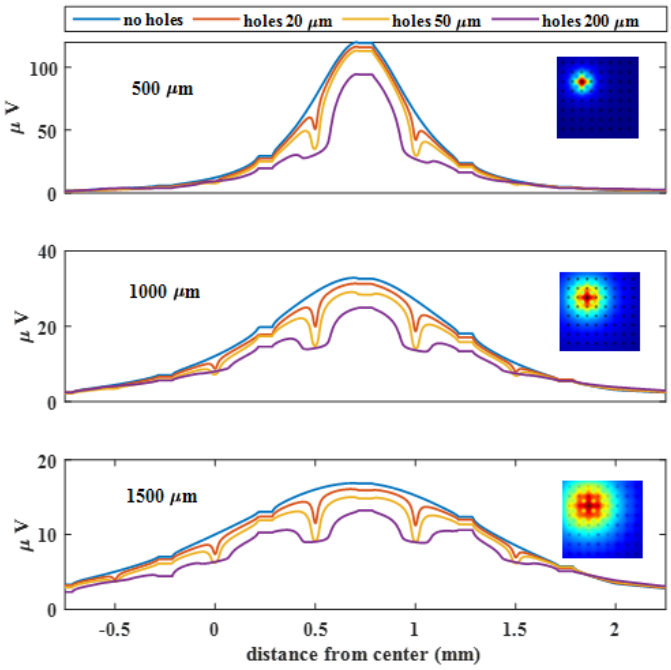

Figure 5.9 Voltage profiles recorded from neurons at three different depths (500 µm, 1000 µm, and 1500 µm), at the bottom surface of the electrode array along the diagonal of the array (4x4 mm) that goes through the centers of the holes and contacts (see Figure 5.10). Each subplot shows voltage profiles for three different sizes of the via holes and for the no-holes case. Note that the color scales are not the same in the insets. The heat map icon attached on the right side of each plot is unique for each position. The maps are specifically for 200 µm hole size and the depth specified on the left.

5.2.3 Spatial Selectivity

For selectivity analysis, two neurons symmetrically positioned along the array diagonal and with varying depths were introduced to the model (Figure 5.10). Spatial selectivity is the ability of an electrode to record preferentially higher signals from one neuron vs. another neuron at a different location. For example, Neuron A positioned precisely below the recording contact will induce a higher amplitude signal on this contact compared to another neuron (Neuron B) placed farther away. Thus, spatial selectivity (SS) is defined as the ratio of the potential difference between the voltages induced by those two neurons to the voltage of the neuron that is located closer to the recording site, Neuron A in this case.

$$SS = \frac{V_A - V_B}{V_A} \qquad \text{Equ. (1)}$$

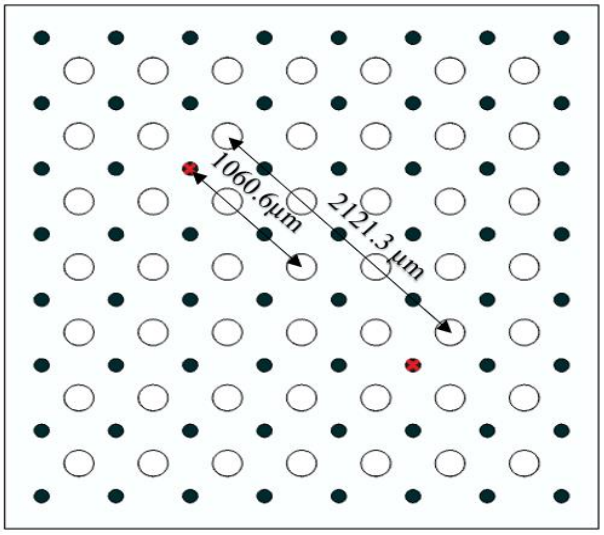

Figure 5.10 Positions of the off-center neurons (red cross) along the diagonal under the electrode array with 8x8 contacts (filled circles). The open circles are the via holes in the substrate. The center-to-center distance between the via holes and the contacts is 353.5 μm in the horizontal and vertical directions.

Next, we tested how spatial selectivity is affected by the hole size for neurons at different depths. Figure 5.11 illustrates the voltages recorded differentially from the two neurons off-centered as shown in Figure 5.10. Spatial Selectivity is defined by Equ. 1 where A and B are the voltages recorded from Neuron A and Neuron B, respectively as marked by black dots in Figure 5.11, by the contact positioned above Neuron B. Each voltage profile is slightly asymmetrical as expected. In this example for a specific neuron depth and hole size, the selectivity is 90%, i.e. the given contact records 90% stronger from Neuron B than Neuron A.

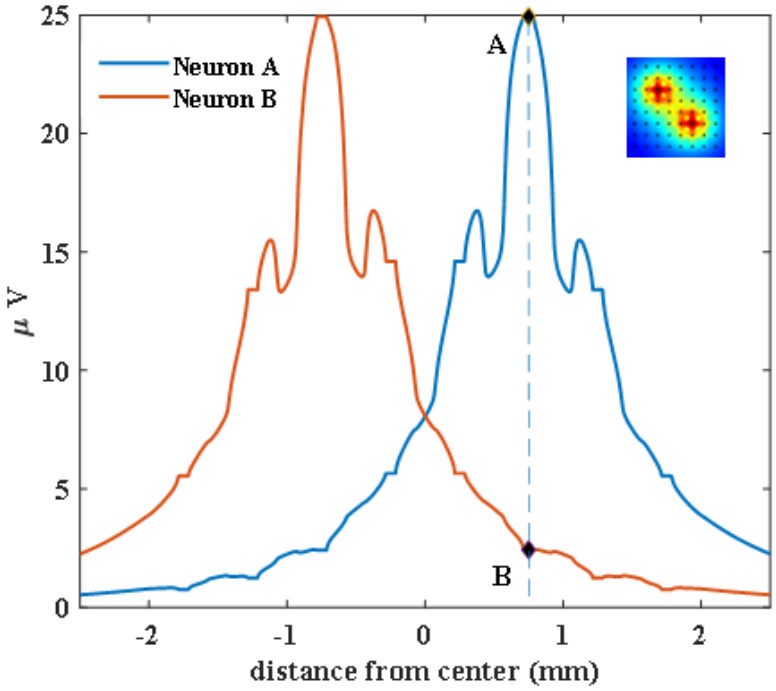

Figure 5.11 Voltage profiles recorded at the bottom surface of the electrode array from two neurons (red and blue) located symmetrically across the array's diagonal line (as in the inset). The blue trace is the voltage detected from Neuron A and the red trace is from Neuron B on the other side. Depths of neurons = 1000 µm, hole sizes = 200 µm. The dash line marks the location of the contact that is directly above the Neurons A (1,060 µm from the center) as shown in Figure 5.10.

As anticipated from the voltage profiles in Figure 5.9, the spatial selectivity is lower for neurons located deeper in the gray matter as the electrode-neuron distance is becoming similar to the inter-neuron distance. The presence of the holes lowers the selectivity with a stronger impact as the hole size is increasing for neuron depths of 500 µm to 1000 µm. Paradoxically, the selectivity increases with increasing hole sizes for the neurons at a depth of 1500 µm.

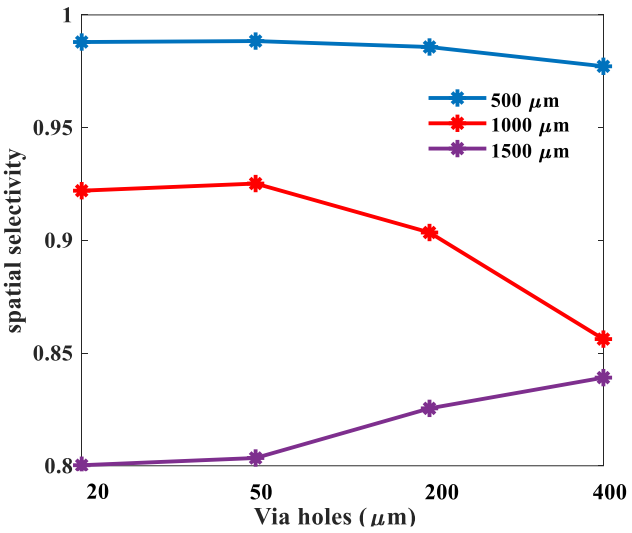

Figure 5.12 Selectivity values calculated for neuron pairs located at different depths (500, 1000, and 1500 µm) with recordings made using the contact located above the Neuron B as shown in Figure 5.10, and for different sizes of the via holes (20, 50, 200 and 400 µm).

CHAPTER 6

DISCUSSION AND CONCLUSION

Substrate Size

The size of the electrode substrate clearly affects the recorded signal amplitudes especially when it is comparable to the array-neuron distance. The signal amplitude saturates once the array dimensions are an order of magnitude larger than the depth of the neuron that is recorded from. In human subjects, the thickness of the gray matter is about 2.6 mm and the human version of the ECoG arrays are usually at least an order of magnitude larger than the deepest targets in the cortex. However, as the brain size is getting smaller in various species like the rat and mouse, the cortex is not becoming proportionally thinner, and sometimes small substrate sizes are preferred to record in small cortical areas. As a practical number, once should be aware that the voltage amplitudes may be reduced more than half (75% compared to a very large array) for substrate dimensions that are in the same order as the depth of the targeted neurons.

Impact of the Holes Size

It is intuitive to expect that the presence of a large via hole in the substrate should cause some reduction of the recorded signals. The simulations of the current study provide some general guidelines as to what size is tolerable for the via holes. The impact evidently depends on the depth of the targeted neurons for recording. As an example, if one is attempting to record from the 5^{th} layer of the motor cortex in the rat, which is where the output pyramidal cells are located at a depth of about 1.5 mm, 200 µm holes will cause about 75% reduction in the recorded signals. That is, a hole size that is 40% of the contact

pitch (500 µm) will attenuate the signals by 75% compared to the substrate without via holes.

Spatial Selectivity

For a neuron at a depth of 500 µm, spatial selectivity is lowered by negligible amounts even at the largest hole size of 400 µm (80% hole diam. / pitch ratio). A significant drop was observed for a neuron at a depth of 1000 µm with increasing hole size above 50 µm. Contrarily, spatial selectivity improved with the hole sizes for the neuron that is at 1500 µm into gray matter. This unexpected trend can be explained by comparing the voltages at the extreme end of profile, away from the neuron position (at the tail end) of the plots in Figure 5.9. Because of the off-center positioning of the neurons, the voltage profiles are asymmetrical. The tail-end voltages near the array center decrease quicker than the ones near the edge for increasing hole sizes (dash circles). This asymmetry at the tails is not as strong for the neuron at 500 µm since the voltage profile is much sharper and the tail-end voltages are near zero. As a result, the selectivity index increases as the voltage recorded from Neuron B is decreasing with the hole size, according to Equ. 1. The hole size at which the selectivity starts increasing will be dependent on the horizontal position of the neurons. For neuron pairs that are closer to the array center, the asymmetry will be less pronounced and so will be the effect of the via holes. Thus, it will take larger holes to make similar increase in selectivity. However, even with this very large hole size in this array, the increase in selectivity was only marginal. Therefore, we do not expect this to be an effective method of achieving spatial selectivity in neural signal recording with array electrodes.

CHAPTER 7

FUTURE STUDIES

The results of this study suggest that selection of the substrate size and the via hole size influence the recorded signal amplitudes to different degrees depending on the depth of the neuron that is recorded from. These design parameters also effect the spatial selectivity of the recordings. Although different ECoG array sizes are used in various species due to the difference in the brain size, the basic principles demonstrated in this project should generalize to those cases as well, including the human version of the arrays.

The FEA can be further improved by inclusion of anisotropy into the white matter, the skull, the scalp, and other layers of the model where it is necessary. Epidural placement of the array may also be considered in future studies. The growth of connective tissue around the electrode in a chronic implant may also introduce significant changes to the recorded signals and the spatial selectivity, which should be included as a design parameter. Because of the small influence it makes in the voltage field, we did not look into the contact size as a design parameter. Future studies may consider, different contact sizes, shapes, and different placements of the via holes with respect to the contacts. Some ECoG electrodes that are commercially available adopted quiet unique geometries, very different than the grid pattern used here, to meet the demands by the users working in different parts of the brain cortex (e.g. auditory cortex). Those designs have to be considered as a separate category with specific designs for each application. Moreover, the presence of blood vessels near the array, which may significantly perturb the recorded voltages, is not considered in the current study. Finally, computational biomechanics can be performed to study parameters like displacement and deformation of the microelectrode array under

pressure changes induced by blood pulsation and respiration, and investigate potential mechanical impact of the electrodes on the cortical tissue for different substrate materials with different a Young's modulus.

APPENDIX A

MATLAB CODE FOR PLOTS IN FIGURE 5.6, 5.7 AND 5.9

```
tab1 = readtable("file location .txt"); %% saves the file in a variable
tab1(1:5,:)=[]; %% removes the text content (headers and titles)
tab1 = removevars(tab1,'Var5'); %% removes extra column
tab1 = sortrows(tab1,'Var1','ascend'); %% sets the table in ascending order with respect to 'Var1' column
x1=tab1{:,1}; %% stores x values from file in x1
y1=tab1{:,2}; %% stores y values from file in y1
m1=find(x1-y1 >= 0 & x1-y1 <= 0.001); %% the data across the diagonal line of array is found
v1=tab1{:,4}; %% stores voltage data for corresponding points in v1
%% same commands repeated for all the simulations to obtain all the dataset %%
figure
plot(x1(m1),v1(m1),x2(m2),v2(m2),x3(m3),v3(m3),x4(m4),v4(m4)); %% plots the voltage values across diagonal line of array for all points of its x axis
xlim([-0.75 2.25]); %% axis data limited for better visualization of selective range
```

APPENDIX B

MATLAB CODE FOR MESH PLOT IN FIGURE 5.8

```
tab1 = readtable("file location .txt"); %% saves the file in a variable
tab1(1:5,:)=[]; %% removes the text content (headers and titles)
tab1 = removevars(tab1,'Var5'); %% removes extra column
x1=tab1{:,1}; %% stores x values from file in x1
y1=tab1{:,2}; %% stores y values from file in y1
v1=tab1{:,4}; %% stores voltage data for corresponding points in v1
x1lin=linspace(min(x1),max(x1)); %% returns a row vector evenly spaced points between maximum and minimum values of x axis
y1lin=linspace(min(y1),max(y1)); )); %% returns a row vector evenly spaced points between maximum and minimum values of y axis
[X1,Y1]=meshgrid(x1lin,y1lin); %% returns 2-D grid coordinates based on the coordinates contained in vectors x and y.
Z1=griddata(x1,y1,v1,X1,Y1); %% interpolation of data values
figure
surf(X1,Y1,Z1) %% mesh plot
```

APPENDIX C

TABLE FOR CALCULATED SELECTIVITY VALUES

Via Holes VS Neuron Depth	20 µm	50 µm	200 µm	400 µm
500 µm	0.987973	0.988401	0.985766	0.9772
1000 µm	0.922026	0.925191	0.903471	0.8562
1500 µm	0.800246	0.803453	0.825467	0.8391

APPENDIX D

MATLAB CODE FOR SELECTIVITY PLOT

```
tab1 = readtable("file location .txt"); %% saves the file in a variable

tab1(1:5,:)=[]; %% removes the text content (headers and titles)

tab1 = removevars(tab1,'Var5'); %% removes extra column

tab1 = sortrows(tab1,'Var1','ascend'); %% sets the table in ascending  order with respect to
'Var1' column

x1=tab1{:,1}; %% stores x values from file in x1

y1=tab1{:,2}; %% stores y values from file in y1

v1 = tab1{:,4}; %% stores voltage data for corresponding points in v1

x2 = (tab1{:,1}; %% stores x values from file in x1

y2 = (tab1{:,2}; %% stores y values from file in y1

v2=v1; %% voltage value would be same for other neuron

x2r = flipud(x2); %% symmetric axis

m1=find(x1-y1 >= 0 & x1-y1 <= 0.001); %% plotting across diagonal line for neuron A

m2=find(x2-y2 >= 0 & x2-y2 <= 0.001); %% plotting across diagonal line for neuron A

figure

plot(x1(m1),v1(m1),x2r(m2),v2(m2)); %% plots 2 voltage traces
```

REFERENCES

1. Shokoueinejad, M., et al., *Progress in the Field of Micro-Electrocorticography.* Micromachines (Basel), 2019. **10**(1).
2. Vidal, J.J., *Toward direct brain-computer communication.* Annu Rev Biophys Bioeng, 1973. **2**: p. 157-80.
3. Hochberg, L.R., et al., *Neuronal ensemble control of prosthetic devices by a human with tetraplegia.* Nature, 2006. **442**(7099): p. 164-71.
4. Krusienski, D.J. and J.J. Shih, *Control of a visual keyboard using an electrocorticographic brain-computer interface.* Neurorehabil Neural Repair, 2011. **25**(4): p. 323-31.
5. Serruya, M.D., et al., *Instant neural control of a movement signal.* Nature, 2002. **416**(6877): p. 141-2.
6. Chapin, J.K., et al., *Real-time control of a robot arm using simultaneously recorded neurons in the motor cortex.* Nat Neurosci, 1999. **2**(7): p. 664-70.
7. Wessberg, J., et al., *Real-time prediction of hand trajectory by ensembles of cortical neurons in primates.* Nature, 2000. **408**(6810): p. 361-5.
8. Rogers, N., et al., *Correlation Structure in Micro-ECoG Recordings is Described by Spatially Coherent Components.* PLoS Comput Biol, 2019. **15**(2): p. e1006769.
9. Insanally, M., et al., *A low-cost, multiplexed muECoG system for high-density recordings in freely moving rodents.* J Neural Eng, 2016. **13**(2): p. 026030-26030.
10. Hollenberg, B.A., et al., *A MEMS fabricated flexible electrode array for recording surface field potentials.* J Neurosci Methods, 2006. **153**(1): p. 147-53.
11. Wang, X., et al., *Mapping the fine structure of cortical activity with different micro-ECoG electrode array geometries.* J Neural Eng, 2017. **14**(5): p. 056004.
12. *CorTec*. Available from: https://www.cortec-neuro.com/company/.
13. *NeuroNexus*. Available from: https://neuronexus.com/.
14. Selvakumaran, J., et al. *Assessing biocompatibility of materials for implantable microelectrodes using cytotoxicity and protein adsorption studies*. in *2nd Annual International IEEE-EMBS Special Topic Conference on Microtechnologies in Medicine and Biology. Proceedings (Cat. No.02EX578)*. 2002.
15. Geninatti, T., et al., *Impedance characterization, degradation, and in vitro biocompatibility for platinum electrodes on BioMEMS.* Biomed Microdevices, 2015. **17**(1): p. 24.
16. Kuzum, D., et al., *Transparent and flexible low noise graphene electrodes for simultaneous electrophysiology and neuroimaging.* Nat Commun, 2014. **5**: p. 5259.
17. Hwang, S.W., et al., *A physically transient form of silicon electronics.* Science, 2012. **337**(6102): p. 1640-4.
18. Yu, K.J., et al., *Bioresorbable silicon electronics for transient spatiotemporal mapping of electrical activity from the cerebral cortex.* Nat Mater, 2016. **15**(7): p. 782-791.
19. Rousche, P.J., et al., *Flexible polyimide-based intracortical electrode arrays with bioactive capability.* IEEE Trans Biomed Eng, 2001. **48**(3): p. 361-71.
20. Geddes, L.A. and L.E. Baker, *The specific resistance of biological material--a compendium of data for the biomedical engineer and physiologist.* Med Biol Eng, 1967. **5**(3): p. 271-93.
21. O'Reilly, M.A., A. Muller, and K. Hynynen, *Ultrasound insertion loss of rat parietal bone appears to be proportional to animal mass at submegahertz frequencies.* Ultrasound Med Biol, 2011. **37**(11): p. 1930-7.

22. J. J. Struijk, J.H., G. Barolat, J. He and H. B. K. Boom, *Paresthesia thresholds in spinal cord stimulation: a comparison of theoretical results with clinical data.* IEEE Transactions on Rehabilitation Engineering, 1993. **1**(2): p. 101-108.
23. Baumann, S.B., et al., *The electrical conductivity of human cerebrospinal fluid at body temperature.* IEEE Trans Biomed Eng, 1997. **44**(3): p. 220-3.
24. Latikka, J., T. Kuurne, and H. Eskola, *Conductivity of living intracranial tissues.* Phys Med Biol, 2001. **46**(6): p. 1611-6.
25. Ranck, J.B., Jr. and S.L. Bement, *The Specific Impedance of the Dorsal Columns of Cat: An Inisotropic Medium.* Exp Neurol, 1965. **11**: p. 451-63.
26. Gasca, F., et al., *Finite element simulation of transcranial current stimulation in realistic rat head model*. 2011. 36-39.
27. Lempka, S., et al., *Theoretical analysis of intracortical microelectrode recordings.* Journal of neural engineering, 2011. **8**: p. 045006.
28. *COMSOL - Software for Multiphysics Simulation*. Available from: https://www.comsol.com/.